Chaos in a dynamic model of traffic flows in an origin-destination network

Xiaoyan Zhang
Department of Civil and Transportation Engineering, Napier University, Edinburgh EH10 5DT, United Kingdom

David F. Jarrett
School of Mathematics and Statistics, Middlesex University, London NW4 4BT, United Kingdom

(Received 5 June 1997; accepted for publication 5 February 1998)

In this paper we investigate the dynamic behavior of road traffic flows in an area represented by an origin-destination (O–D) network. Probably the most widely used model for estimating the distribution of O–D flows is the gravity model, [J. de D. Ortuzar and L. G. Willumsen, *Modelling Transport* (Wiley, New York, 1990)] which originated from an analogy with Newton's gravitational law. The conventional gravity model, however, is static. The investigation in this paper is based on a dynamic version of the gravity model proposed by Dendrinos and Sonis by modifying the conventional gravity model [D. S. Dendrinos and M. Sonis, *Chaos and Social-Spatial Dynamics* (Springer-Verlag, Berlin, 1990)]. The dynamic model describes the variations of O–D flows over discrete-time periods, such as each day, each week, and so on. It is shown that when the dimension of the system is one or two, the O–D flow pattern either approaches an equilibrium or oscillates. When the dimension is higher, the behavior found in the model includes equilibria, oscillations, periodic doubling, and chaos. Chaotic attractors are characterized by (positive) Liapunov exponents and fractal dimensions. © *1998 American Institute of Physics.*
[S1054-1500(98)00302-4]

Road traffic in an area can be characterized by aggregate flows from their origins to their destinations. The distribution of origin–destination (O–D) flows in an area is an important source of information for traffic management and control in the short term, as well as for transport planning and highway design in the longer term. Probably the most widely used model for predicting traffic flows between each O–D pair is the gravity model, [J. de D. Ortuzar and L. G. Willumsen, *Modelling Transport* (Wiley, New York, 1990)] which originated from an analogy with Newton's gravitational law. The conventional gravity model, however, is static, although traffic flows are bound to vary with time. A static model considers only an equilibrium state of a traffic system, making the implicit assumption that the equilibrium is stable. Equilibrium and stability are most important and desirable in a traffic system. However, whether or not an equilibrium will prevail in the system depends on road and traffic conditions. Variations in these will tend to push the system away from the equilibrium. The system can then be expected to move toward another attractor which may not even be an equilibrium. The model that will be investigated in this paper is the dynamic version of the gravity model proposed by Dendrinos and Sonis [D. S. Dendrinos and M. Sonis, *Chaos and Social-Spatial Dynamics* (Springer-Verlag, Berlin, 1990)]. It models the variations of O–D flows in an area over discrete-time periods, such as each day, each week, and so on. By investigating the model under various conditions represented by different parameter values, we are able to understand different types of behavior, particularly disequilibrium behavior, in the traffic system.

I. INTRODUCTION

Road traffic flows can be modeled at different levels of spatial scope: an area level, a road network level, and a road link level. In transport modelling, the area under consideration is divided into sub-areas called *zones*. A journey from one zone to another is called a *trip*. A particular zone may be an origin, or a destination, or both if trips can both start and terminate there. A zone is normally represented by a single point called its *centroid* and trips from and to the zone are assumed concentrated at the centroid. Thus, the area can be represented by an origin–destination (*O–D*) *network*, with the nodes being the centroids and the arcs being the connections between O–D pairs. Each O–D pair is connected by one or more *routes*, that is, chains of road links. An O–D network is therefore an aggregate representation of the actual road network in the area.

Four transport models are used to estimate successively the distribution of traffic flows on a road network in an area. (1) *Trip generation*, in which the numbers of trips generated from and attracted to each zone are determined given the socio-economic data in the area. (2) *Trip distribution*, in which the number of trips between each O–D pair is estimated. (3) *Modal split*, which splits trip makers into the alternative transport modes available, typically between private cars and public buses. (4) *Trip assignment*, which assigns trips between each O–D pair to alternative routes connecting these O–D pairs, so that the traffic flows on each

TABLE I. A general form of a trip matrix.

Origin		Destination 1	2	⋯	j	⋯	J	Total Σ_j
1		x_{11}	x_{12}	⋯	x_{1j}	⋯	x_{1J}	o_1
2		x_{21}	x_{22}	⋯	x_{2j}	⋯	x_{2J}	o_2
⋯								
i		x_{i1}	x_{i2}	⋯	x_{ij}	⋯	x_{iJ}	o_i
⋯								
I		x_{I1}	x_{I2}	⋯	x_{Ij}	⋯	x_{IJ}	o_I
Total	Σ_i	d_1	d_2	⋯	d_j	⋯	d_J	$X=1$

road link can be obtained. These route/link flows may then be used for traffic congestion prediction, traffic signal setting, road designing, and so on. The gravity model was developed for trip distribution. It models traffic flows at the O–D network level without concerning itself with which specific routes the O–D flows take—there may be more than one route connecting an O–D pair.

The O–D flow pattern in an area is represented by a *trip matrix*. This is essentially a two-dimensional array of cells where each row corresponds to an origin and each column to a destination, as shown in Table I. In this table, x_{ij} is the number of trips from zone i to zone j, o_i is the total number of trips originating in zone i, d_j is the total number of trips attracted to zone j, X is the total number of trips from all origins or to all destinations, I is the number of origins, and J is the number of destinations. The relationship between the entries of the matrix and the marginal totals can be expressed as

$$\Sigma_j x_{ij} = o_i, \quad i = 1,2,\ldots,I, \tag{1a}$$

$$\Sigma_i x_{ij} = d_j, \quad j = 1,2,\ldots,J. \tag{1b}$$

For the convenience of the analysis and description, we shall consider relative quantities of trips. In other words, we assume

$$\Sigma_{ij} x_{ij} = 1. \tag{1c}$$

Clearly, we must then have $\Sigma_i o_i = 1$ and $\Sigma_j d_j = 1$ as well. The marginal totals o_i and d_j are normally estimated by a trip generation model and can be used as inputs to a trip distribution model, which in turn gives the entries of a trip matrix. If a trip distribution model satisfies both (1a) and (1b), in other words, if the total number of trips originating and terminating in each zone given by the model equals the predetermined totals, then the model is said to be *doubly constrained*. If a model satisfies (1a) or (1b) but not both then it is *origin constrained* or *destination constrained*. These models are also called *singly constrained* models. If a model satisfies neither set of constraints, it is called an *unconstrained* model, although the normalization condition (1c) must still be fulfilled. Which type of constraint should be involved in a model depends mainly on the availability of information about the o_i and d_j. Other factors may also be considered. For example, for non-work trips such as trips for shopping, the total number of trips from an origin (for example, a residential area) may be regarded as fixed while the total number of trips to a destination (for example, a city center) should be considered to be variable. In this case, an origin-constrained model may be suitable. That the total flow attracted to each zone is known does not necessarily mean that a doubly constrained model should be used.

Associated with each O–D pair there is a travel cost. It may be measured in terms of distance, time or monetary units, or a combination of these. It is normally referred to as the *generalized cost of travel*. In the gravity model, the number of trips between each O–D pair is determined based on the cost through a *deterrence function* which relates the number of trips to the cost. For example, in one of the earliest doubly constrained gravity models, it was assumed, following Newton's gravitational law, that the number of trips between each O–D pair is proportional to o_i and d_j, and is inversely proportional to the square of the distance between the O–D pair. In this model, the deterrence function is a power function with the power of -2. More general types of deterrence function have been considered,[1] including an exponential function, a power function, and a combined exponential and power function. The exponential and power deterrence functions are both decreasing functions of costs. The combined function is not a monotonic function of cost; the number of trips first increases and then decreases with the cost. It has been observed that, in the case of motorized trips, the combined function can fit the data better than the other two functions. This is because comparatively few people use cars for very short trips while the power and exponential functions cannot reproduce this feature.

The history of the family of gravity models can be traced back to over one century ago. However, it was not until the 1950s that the model was applied to the trip distribution. The model provides a rigorous tool for modeling and analyzing transport network problems in a fairly simple mathematical form. Apart from the trip distribution, the gravity model has also been used in another closely related transport problem, namely, the *trip matrix estimation* problem.[1] This is an alternative way of estimating a trip matrix, but from traffic count data on road links. The trip matrix estimation problem may be considered as a dual of trip assignment problems—the input of one problem is the output of the other.

The conventional gravity model is static with travel costs independent of traffic flows. This may be based on two assumptions. First, the underlying traffic system would stick to an equilibrium state defined by the model. In general, however, an equilibrium may not be the only possible type of steady state of a dynamical system; there may also be other types of steady states, such as oscillations or chaos. In addition, any equilibrium need not be unique, nor always stable. Secondly, the effects of congestion are negligible in the system. In practice, the costs will normally increase with flows because of congestion effects.

In recent years, there have been many dynamic analyses of trip assignment models and trip matrix estimation models, but hardly any dynamic considerations of the gravity models for a trip distribution. Dendrinos and Sonis introduced iterative dynamics to the conventional gravity model.[2] In the dynamic gravity model, the O–D flows at each time period are generated from the travel costs at the previous time period and the travel costs are assumed to be a function of O–D flows.

Dendrinos and Sonis suggested that the dynamic gravity model had a potential to show interesting behavior such as chaos, but they did not give any detailed analysis. An unconstrained version of this model was investigated by Jarrett and Zhang.[3] It was found that a gravity model with the exponential or the power deterrence function can have only point attractors and period-2 attractors. With the combined deterrence function, the model was found to be chaotic for some values of parameters in the model. On the other hand, the existence, uniqueness and the stability of an equilibrium in the dynamic gravity model have been analyzed by Zhang and Jarrett,[4] where multiple equilibria were identified.

In this paper, the dynamic gravity model, including the unconstrained, singly constrained and doubly constrained versions, is investigated. We shall concentrate on models with the combined deterrence function and on identifying different types of attractors in the model. Different initial conditions and parameter values will be considered; the chaotic behavior found in the model will be characterized by Liapunov exponents and fractal dimensions. The model is described in the next section, which is followed by the numerical analysis of the model in the subsequent section. Liapunov exponents and fractal dimensions for chaotic attractors are calculated in the fourth section. The paper is summarized in the last section. For briefness the term ''gravity model'' means the dynamic gravity model unless otherwise stated.

II. THE MODEL

Let $\mathbf{x}$ be a trip matrix with x_{ij} being the number of trips from origin i to destination j. Denote the set of all possible values of $\mathbf{x}$ by S. This will be defined by non-negativity constraints on the x_{ij} and appropriate marginal constraints. Then the dynamic gravity model is defined by a mapping,[2]

$$\mathbf{F}: \ S \to S, \quad F_{ij}(\mathbf{x}) = \psi_{ij}(\mathbf{x}) f(c_{ij}(x_{ij})),$$
$$i = 1,2,\ldots,I, \quad j = 1,2,\ldots,J, \tag{2}$$

where $\psi_{ij}(\mathbf{x})$ is an appropriate normalizing factor determined from the marginal constraints, c_{ij} is the travel cost, which is normally assumed to be an increasing function of x_{ij}, $f(\cdot)$ is the deterrence function. The map (2) defines a discrete-time dynamical system: if n is the discrete time, and $\mathbf{x}(n)$ the O–D flow pattern at time n, then $\mathbf{x}(n+1) = \mathbf{F}(\mathbf{x}(n))$ is the O–D flow pattern at time $n+1$. For nonwork trips, such as trips for shopping, we may consider the variations of O–D flows over time periods like each day or each week because the number of trips between each O–D pair is the result of daily or weekly decisions of trip makers. For work trips, on the other hand, a longer time slice may be more appropriate since the choices of origins (for example, residence locations) and/or destinations (for example, the work place) are normally based on longer-term decisions.

In order to model the congestion effect between each O–D pair, Dendrinos and Sonis suggested the following cost function:[2]

$$c_{ij}(x_{ij}) = c_{ij}^0[1 + \alpha(x_{ij}/q_{ij})^\gamma],$$

where c_{ij}^0 is the uncongested travel cost from origin i to destination j, q_{ij} is the corresponding capacity of the roads (the ability that roads can accommodate traffic flows), and α and γ are positive constants. In this function, the minimum function value is the uncongested cost at $x_{ij} = 0$. When $x_{ij} > 0$, the cost increases with the flow.

The deterrence function is a generalized function of travel costs with one or more parameters for calibration. The three types of deterrence functions mentioned in the Introduction can be written as[1]

$$f(c_{ij}) = c_{ij}^\mu \exp(-\beta\, c_{ij}),$$

where μ and β are parameters. When $\mu = 0$ and $\beta > 0$, f is an exponential deterrence function; when $\mu < 0$ and $\beta = 0$ it is a power deterrence function; and when $\mu > 0$ and $\beta > 0$ it is a combined deterrence function. The parameters are estimated so that the model reproduces, as close as possible, the observed trip length (cost) distribution, or the distribution of the number (or equivalently the frequency) of trips over travel costs.

The normalizing factor $\psi_{ij}(\mathbf{x})$ in (2) is chosen so that one or more of the marginal constraints (1a)–(1c) are satisfied. We can have three types of models with different constraints, as follows.

(1) Unconstrained model:

$$F_{ij}(\mathbf{x}) = \frac{f(c_{ij}(x_{ij}))}{\Sigma_{kl} f(c_{kl}(x_{kl}))}, \quad x_{ij} \geqslant 0, \quad \sum_{ij} x_{ij} = 1.$$

(2) Singly-constrained model. There are two types: the origin-constrained model,

$$F_{ij}(\mathbf{x}) = o_i \frac{f(c_{ij}(x_{ij}))}{\Sigma_l f(c_{il}(x_{il}))}, \quad x_{ij} \geqslant 0, \quad \sum_j x_{ij} = o_i;$$

and the destination-constrained model,

$$F_{ij}(\mathbf{x}) = d_j \frac{f(c_{ij}(x_{ij}))}{\Sigma_k f(c_{kj}(x_{kj}))}, \quad x_{ij} \geqslant 0, \quad \sum_i x_{ij} = d_j.$$

(3) The doubly constrained model. In a doubly constrained model, the normalizing factor is replaced by two sets of constants, $a_i(\mathbf{x})$ and $b_j(\mathbf{x})$. The model is

$$F_{ij}(\mathbf{x}) = a_i(\mathbf{x}) b_j(\mathbf{x}) f(c_{ij}(x_{ij})),$$
$$x_{ij} \geqslant 0,$$
$$\sum_i x_{ij} = d_j, \quad \sum_j x_{ij} = o_i, \tag{3a}$$

where $a_i(\mathbf{x})$ and $b_j(\mathbf{x})$ satisfy the equations

$$a_i(\mathbf{x}) = \frac{o_i}{\Sigma_j b_j(\mathbf{x}) f(c_{ij}(x_{ij}))}, \tag{3b}$$

$$b_j(\mathbf{x}) = \frac{d_j}{\Sigma_i a_i(\mathbf{x}) f(c_{ij}(x_{ij}))}. \tag{3c}$$

Clearly the state space of the unconstrained model has dimension $I \times J - 1$. It can be seen that in the origin-constrained model F_{ij} depends only on the elements of the ith row of trip matrix $\mathbf{x}$. Therefore the model consists of I independent equations. Each equation, after further normalization by dividing each element of the trip matrix by o_i, is

equivalent to the unconstrained model with a dimension $J-1$. Similarly, the destination-constrained model consists of J independent equations and each component of the model can be normalized to get a model equivalent to the unconstrained model with a dimension $I-1$. Therefore, the unconstrained and singly constrained models can be written in the more general form, using single subscripts for simplification,

$$F_i(\mathbf{x}) = \frac{f(c_i(x_i))}{\Sigma_k f(c_k(x_k))},$$

$$x_i \geqslant 0, \quad \sum_i x_i = 1, \quad i = 1,2,\ldots,K, \tag{4}$$

where

$$c_i(x_i) = c_i^0[1+\alpha(x_i/q_i)^\gamma], \quad i = 1,2,\ldots,K,$$

$$f(c_i) = c_i^\mu \exp(-\beta c_i), \quad i = 1,2,\ldots,K.$$

When $K = I \times J$ the equation represents an unconstrained dynamic gravity model; while when K equals I or J the equation represents one component of a singly constrained model with o_i or d_j being set to 1 for normalization. A doubly constrained model, however, is different. The model has a state space of dimension $(I-1)\times(J-1)$ and it contains two sets of parameters $a_i(\mathbf{x})$ and $b_j(\mathbf{x})$ which are interdependent. This will be discussed further in the numerical investigations.

In the numerical calculations in the next section, different initial conditions and parameter values will be considered while all other conditions, including the uncongested travel cost and capacity of each O–D pair, and the marginal totals in the doubly constrained model will be assumed to be given. The analysis of the unconstrained or singly constrained model will be based on the generalized form (4) and the doubly constrained model will be investigated separately.

III. NUMERICAL INVESTIGATIONS

A. Unconstrained or singly constrained model

Given an initial condition and the values of parameters, the gravity model (4) can be iterated until a steady state or an attractor is reached. It was found that when the number of dimensions is 1 or 2, the system either converges a fixed point or approaches a period-2 orbit. When the dimension is higher (3 or more), however, more complicated behavior occurs in the model. Period doubling and apparently irregular behavior or chaos were found to be quite typical. The phase portrait projection of a chaotic attractor found in a model of two origins and two destinations is shown in Fig. 1(a), where it can be seen that the attractor is geometrically a very complicated object. When the initial condition is changed slightly, the orbit will soon diverge. Sensitive dependence on initial conditions is shown in Figure 1(b), where the solid line is the series starting at $\mathbf{x}=[0.0300\ 0.3521\ 0.5313\ 0.0866]$, while the dashed line is the series starting at $\mathbf{x}=[0.0301\ 0.3520\ 0.5313\ 0.0866]$. The starting time is $n=1000$. It can be seen that the orbits distinguish themselves after less than 20 iterations.

More features of the dynamic behavior in the model can be found by the use of bifurcation diagrams. These are produced by increasing the bifurcation parameter step by step and, at each step, iterating the model until an attractor is reached. When producing these diagrams, the initial conditions were taken in two ways. One way is simply to use the same initial conditions for all steps of the parameter and the other to use the final states of the system at the previous step of the parameter, given the initial condition at the first step. There may be a longer transient in the first method than in the second. By starting from different initial conditions, different attractors may be detected if there is more than one attractor for the same value of the parameter. Figures 2–3 are two sets of bifurcation diagrams for β but with different values of μ. Each set contains two diagrams with two ways of starting. Figures 4(a)–4(b) are local enlargements of Figures 3(a)–3(b), respectively, showing the bifurcation sequences in more detail. For example, there is a *periodic window* when β is approximately between 3.15 and 3.18 in Figure 4(a).

Two important features can be seen in these bifurcation diagrams. First, there are some discontinuous points in Figs. 2(a), 3(a), and 4(a). The reason for this is the existence of multiple attractors in the state space. As the bifurcation parameter varies, the basins of attractors vary too. Iterations from the same initial conditions may converge to different attractors for different values of the parameter. When the initial condition is the final state of the system at the previous step of the parameter, as in Figs. 2(b), 3(b), and 4(b), the system is more likely to approach the same attractor at successive steps of the parameter because the increment of the parameter is very small. The multiplicity of attractors is also confirmed by the fact that in Figs. 2–3, different starting points lead to different bifurcation sequences and different sets of attractors.

The second feature in the bifurcation diagrams is that there seems to be a typical bifurcation sequence. As the value of parameter increases, the system starts with an equilibrium, followed by a *period doubling* sequence. With the exception of Fig. 2(b), the period doubling sequence leads to chaos. In Fig. 2(b), there is the period doubling up to 16 and then undoubling to period 2 without going through chaos. What is more, chaotic behavior is also followed by periodic undoubling, to a periodic orbit. This behavior may be explained by the form of the deterrence function. As was mentioned in the Introduction, a previous study by Jarrett and Zhang[3] indicated that with the exponential and power deterrence functions, the gravity model will have only point attractors and period-2 attractors. Both types of deterrence function are monotonic decreasing functions. The combined deterrence function is not monotonic and has a maximum at $c=\mu/\beta$. For a fixed value of μ, as $\beta \to 0$, the function tends to an increasing function. This is clearly not a suitable deterrence function. As β increases gradually, the position of the maximum moves to the left, and the function becomes a decreasing function in the limit. The typical bifurcation sequence of the model is equilibrium$\to$periodic doubling and chaos $\to$ period-2 orbit as β increases. This seems to indicate that it is the non-monotonic nature of the deterrence function that causes complicated behavior in the gravity

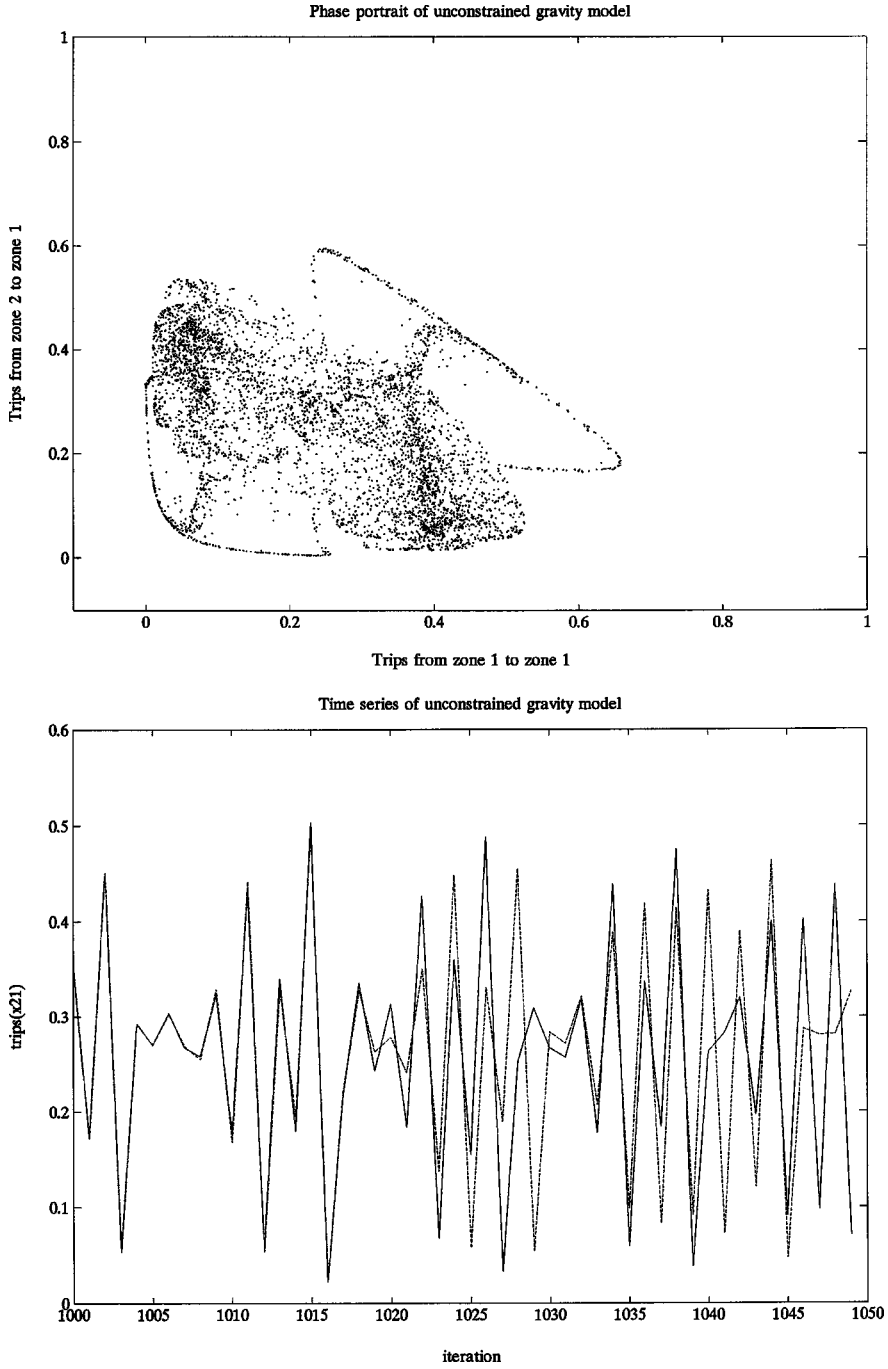

FIG. 1. Chaotic attractor of the unconstrained or singly constrained gravity model, with $\mu = 8.0$, $\beta=3.25$, $\alpha=1.0$, $\gamma=1.0$. (a) Phase portrait projection; (b) sensitive dependence on initial conditions.

model. It also appears that the model can have only simple attractors such as equilibrium and period-2 orbit if the deterrence function is monotonic. It is easy to prove this result in the one-dimensional case, although we have not been able to prove it in higher dimensions.

B. The doubly constrained model

The doubly constrained model cannot be iterated directly like the unconstrained or singly constrained model, because it contains two sets of parameters $a_i(\mathbf{x})$ and $b_j(\mathbf{x})$ which are interdependent. The calculation of one set needs the values of the other set. This suggests an iteration process. The method from Ortúzar and Willumsen[1] will be used here. Given the values of deterrence functions for each O–D pair, $f(c_{ij})$, the algorithm in outline is as follows:

(1) Set all $b_j(\mathbf{x})=1.0$ and find $a_i(\mathbf{x})$'s by (1a) that satisfy the origin constraints.
(2) With the latest $a_i(\mathbf{x})$'s and by (1b), find $b_j(\mathbf{x})$'s which satisfy the destination constraints.
(3) Keeping the $b_j(\mathbf{x})$'s fixed, calculate $a_i(\mathbf{x})$'s, again by (1a).
(4) Repeat steps (2) and (3) until convergence is achieved.

Once the $a_i(\mathbf{x})$'s and $b_j(\mathbf{x})$'s are determined, the

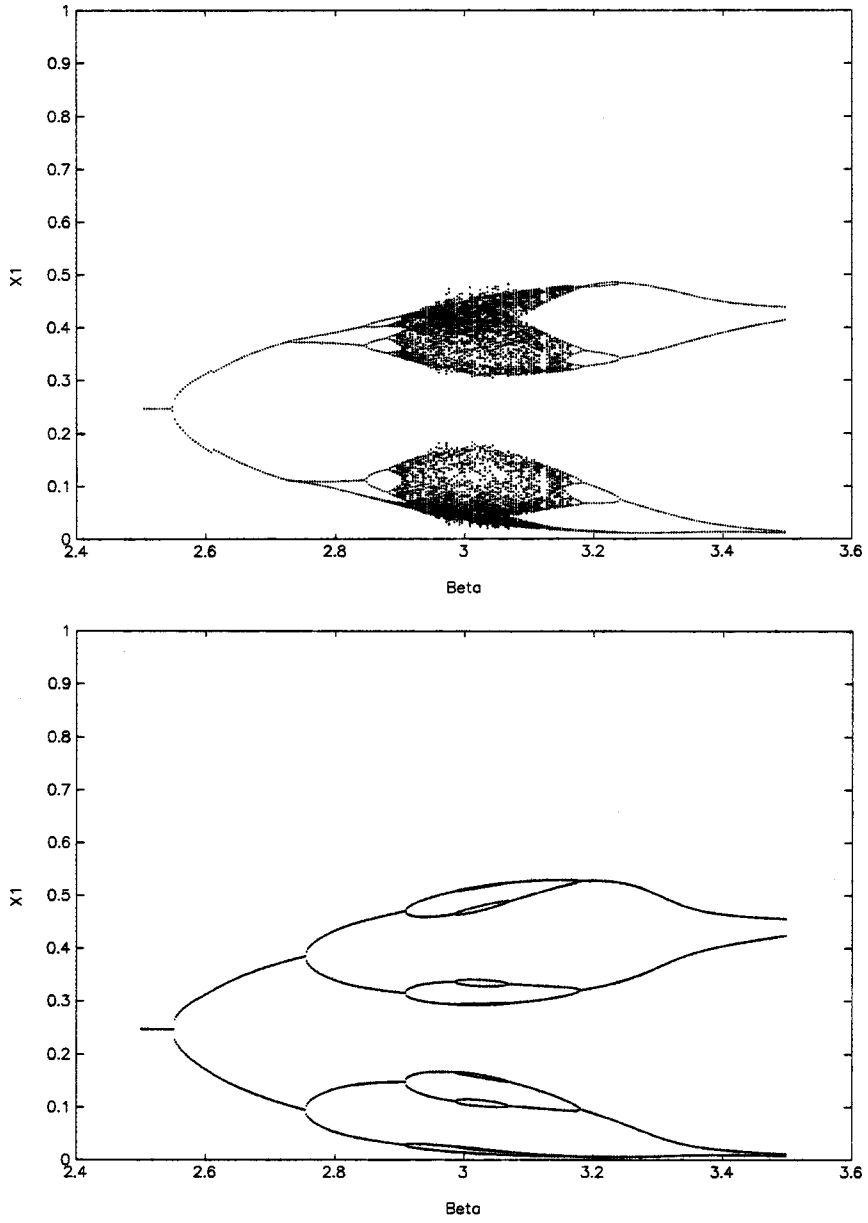

FIG. 2. Bifurcation diagram of the unconstrained or singly constrained gravity model for β, with $\mu=7.0$, $\alpha=1.0$, $\gamma=1.0$. (a) Initial conditions are the same for all values of β; (b) initial conditions are the final states of the previous step of β.

$F_{ij}(\mathbf{x})$'s can be obtained by (3a). Thus the numerical calculations of the doubly constrained model involve two nested iterations. The inner iteration is the one outlined above to obtain $a_i(\mathbf{x})$'s and $b_j(\mathbf{x})$'s so as to get $F_{ij}(\mathbf{x})$'s; the outer iteration is $\mathbf{x}(n+1)=\mathbf{F}(\mathbf{x}(n))$, made for n.

Numerical calculations showed that the dynamic behavior in the doubly constrained model is similar to that in the unconstrained or singly constrained models. When the dimension is lower, there are still only point and period-2 attractors. When the dimension is higher (4 or more), the behavior is more complicated. Chaos was found to exist widely in the model. Figures 5(a)–5(b) show one of the chaotic attractors found in a model of three origins and three destinations. The time series appears to be even more irregular than that for the chaotic attractor in the unconstrained or singly constrained model [Figure 1(b)]. The power spectrum is continuous, implying the motion is chaotic.

Bifurcation diagrams were produced for the four parameters α, γ, μ and β in the model and for models with up to four origins and four destinations. The diagrams are, again, more complicated than those for the unconstrained or singly constrained model. There does not seem to be an obvious periodic doubling sequence or any other clear bifurcation route in the diagrams. The reason for the more irregular behavior in the doubly constrained gravity model may be that the model and the state space are more complicated. The unconstrained or singly constrained model is a mapping of a simplex onto itself while the domain of a doubly constrained model is an $(I-1)(J-1)$-dimensional closed convex subset of a Cartesian product of simplexes.

IV. CHARACTERIZATION OF CHAOTIC BEHAVIOR

In this section, chaotic behavior found in the gravity model is examined by Liapunov exponents and fractal di-

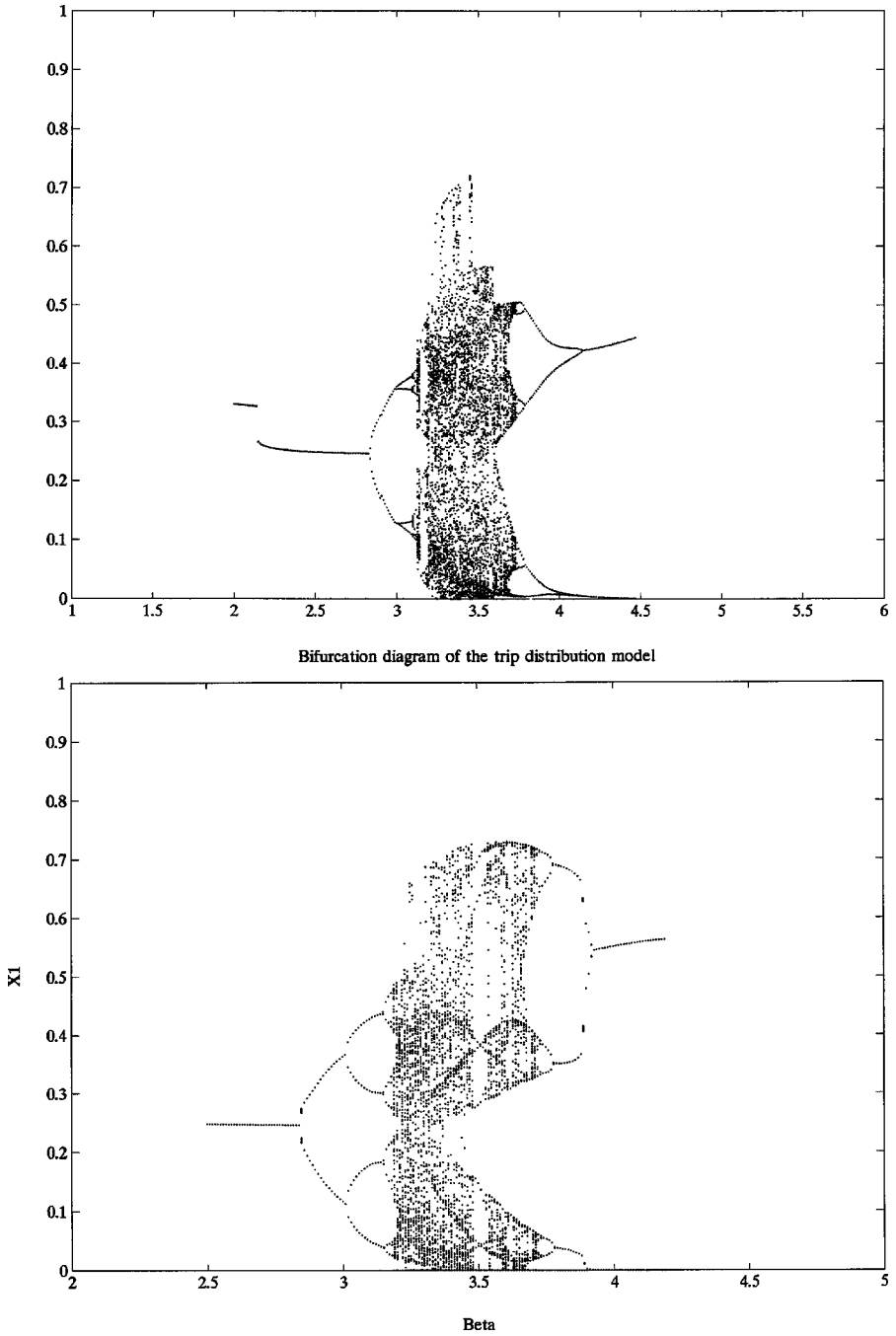

FIG. 3. Bifurcation diagram of the unconstrained or singly constrained gravity model for β, with $\mu=8.0$, $\alpha=1.0$, $\gamma=1.0$. (a) Initial conditions are the same for all values of β; (b) initial conditions are the final states of the previous step of β.

mensions. The algorithms for calculating the two measures adopted here will be outlined briefly and then applied to the gravity models. The programs developed were tested by calculating the two measures of a chaotic attractor of the well-known Hénon map[5] and good agreements with those in the literature[6,7] were obtained.

A. Liapunov exponents

Chaotic attractors are the attractors with sensitive dependence on initial conditions.[8] The divergence of neighboring trajectories can be measured by positive *Liapunov exponents*. Consider the gravity model $\mathbf{x}(n+1)=\mathbf{F}(\mathbf{x}(n))$. Let $\mathbf{J}(\mathbf{x})$ be the Jacobian matrix of $\mathbf{F}(\mathbf{x})$ at $\mathbf{x}\in S$: $\mathbf{J}(\mathbf{x})=\partial\mathbf{F}(\mathbf{x})/\partial\mathbf{x}$. Denote the Jacobian matrix $\partial\mathbf{F}^{(n)}(\mathbf{x})/\partial\mathbf{x}$ of the nth iteration $\mathbf{F}^{(n)}(\mathbf{x})$ by $\mathbf{J}$. Then, by the chain rule of differentiation we have

$$\mathbf{J}=\mathbf{J}(\mathbf{F}^{(n-1)}(\mathbf{x}))\cdots\mathbf{J}(\mathbf{F}(\mathbf{x}))\mathbf{J}(\mathbf{x}), \tag{5}$$

where $\mathbf{J}(\mathbf{F}^{(m)}(\mathbf{x}))$ is the Jacobian matrix of $\mathbf{F}$ evaluated at the point $\mathbf{F}^{(m)}(\mathbf{x})$. Let σ_i be the ith eigenvalue of the matrix,

$$\lim_{n\to\infty}[\mathbf{J}^*\mathbf{J}]^{1/2n},$$

where $\mathbf{J}^*$ stands for the transpose of $\mathbf{J}$. Then the ith Liapunov exponent is defined as[8]

$$\lambda_i=\mathrm{Log}|\sigma_i|.$$

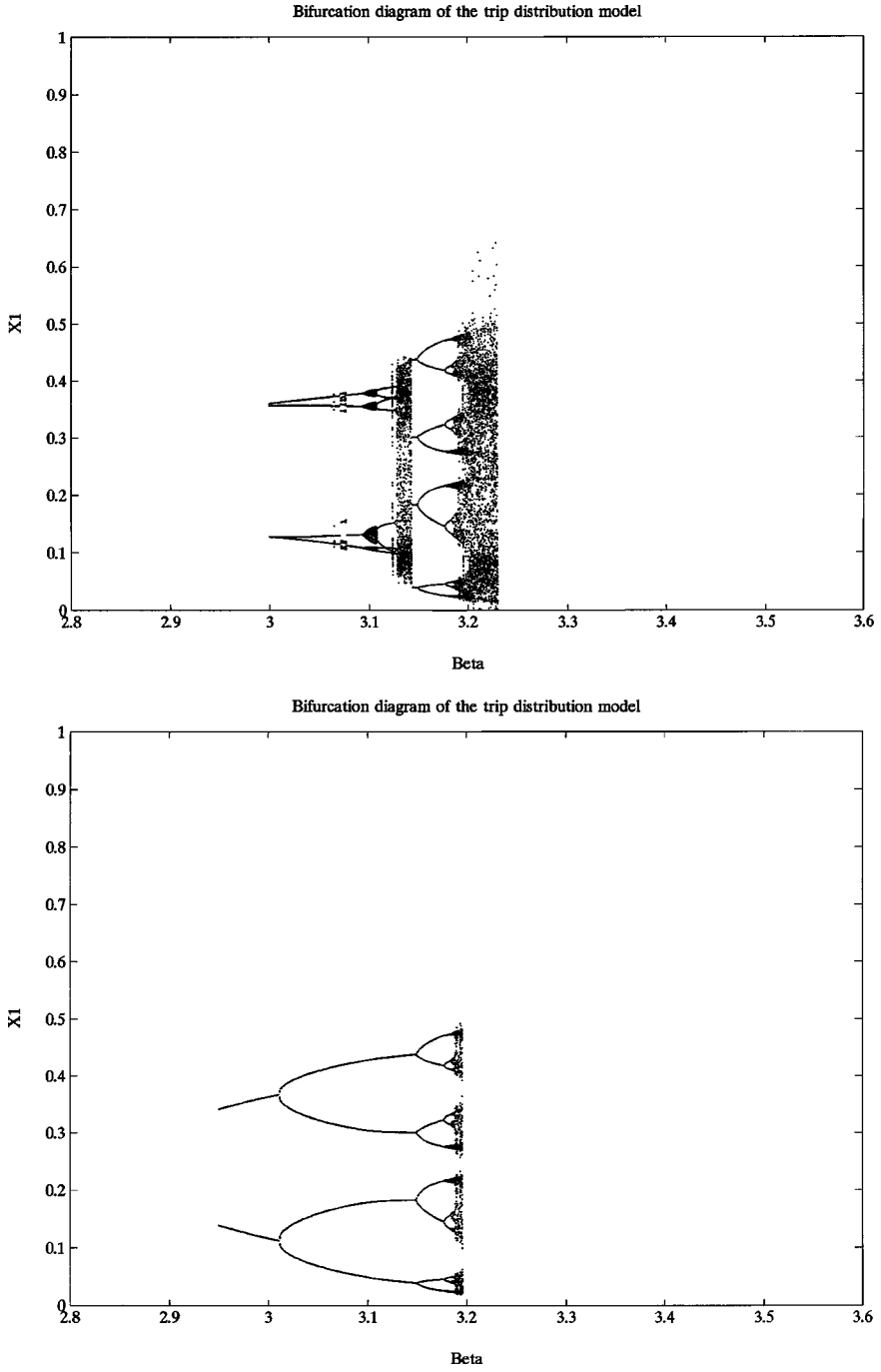

FIG. 4. Enlargements of Figs. 3(a)–3(b). (a) Enlargement of Fig. 3(a); (b) enlargement of Fig. 3(b).

Two methods for calculating Liapunov exponents have been suggested by Wolf *et al.*[9] and Eckmann and Ruelle,[8] respectively. The second algorithm, which involves calculating the product (5) by QR factorizations, is usually preferred[6] and is used here. The algorithm can be used directly to calculate the Liapunov exponents for the unconstrained or the singly constrained gravity model. Liapunov exponents for the chaotic attractor shown in Fig. 1 were calculated. The three exponents were found to be $[0.20-0.02-0.70]$, with the first one being positive. Shown in Fig. 6 is the first Liapunov exponent against β with the same values of parameters as those in Fig. 2(a). The second and the third exponents are both negative. By comparing Fig. 6 with Fig. 2(a) it can be seen that the first exponent is negative for nonchaotic attractors and is positive for chaotic ones.

For the doubly constrained gravity model, the partial derivatives in the Jacobian matrix need to be calculated numerically because the two sets of normalizing factors in the model are interdependent. Consider the doubly constrained model (3). The partial derivatives can be found to be

$$\frac{\partial F_{ij}}{\partial x_{kl}} = b_j(\mathbf{x}) f(c_{ij}(x_{ij})) \frac{\partial}{\partial x_{kl}} a_i(\mathbf{x}) + a_i(\mathbf{x}) f(c_{ij}(x_{ij})) \frac{\partial}{\partial x_{kl}} b_j(\mathbf{x}) + a_i(\mathbf{x}) b_j(\mathbf{x}) \frac{\partial}{\partial x_{kl}} f(c_{ij}(x_{ij})), \tag{6}$$

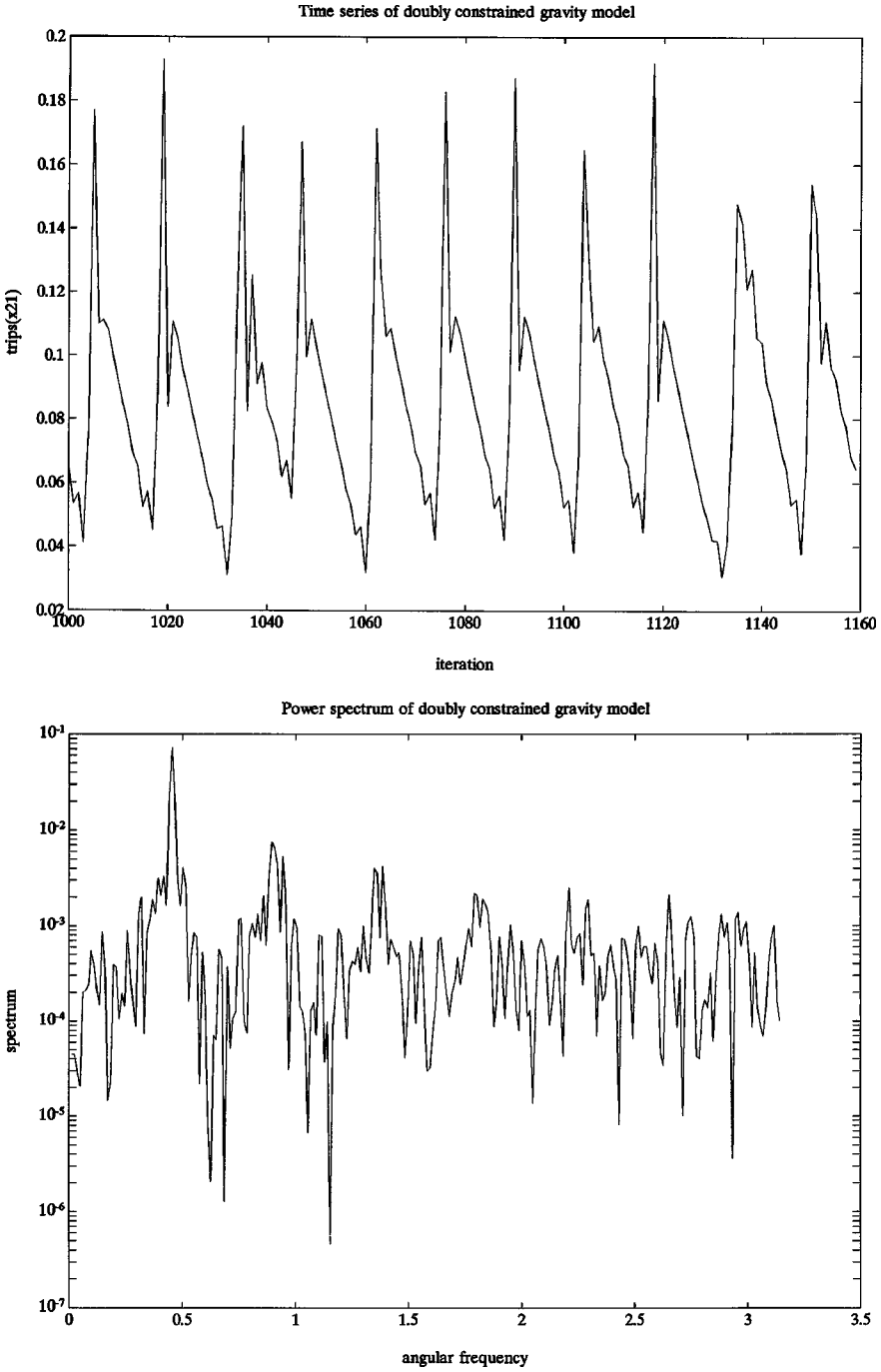

FIG. 5. Chaotic attractor of the doubly constrained gravity model, with $\mu=4.5$, $\beta=1.25$, $\alpha=1.5$, $\gamma=1.5$. (a) Number of trips from origin 2 to destination 1; (b) power spectrum.

where

$$\frac{\partial}{\partial x_{kl}} f(c_{ij}(x_{ij})) = \begin{cases} \dfrac{\mathrm{d}}{\mathrm{d}x_{kl}} f(c_{kl}(x_{kl})), & \text{if } i=k, \quad j=l, \\ 0, & \text{otherwise.} \end{cases}$$

By equations (3b) and (3c), the partial derivatives $\partial a_i(\mathbf{x})/\partial x_{kl}$ and $\partial b_j(\mathbf{x})/\partial x_{kl}$ should satisfy

$$\frac{\partial}{\partial x_{kl}} a_i(\mathbf{x}) = \frac{o_i}{\left(\Sigma_j b_j(\mathbf{x}) f(c_{ij}(x_{ij}))\right)^2} \times \sum_j \left[f(c_{ij}(x_{ij})) \frac{\partial}{\partial x_{kl}} b_j(\mathbf{x}) + b_j(\mathbf{x}) \frac{\partial}{\partial x_{kl}} f(c_{ij}(x_{ij})) \right],$$

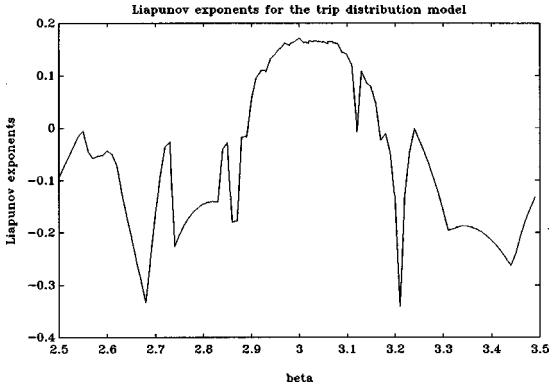

FIG. 6. The first Liapunov exponents against β for the unconstrained or singly constrained gravity model.

$$\frac{\partial}{\partial x_{kl}} b_j(\mathbf{x}) = \frac{d_j}{\left(\Sigma_i a_i(\mathbf{x}) f(c_{ij}(x_{ij}))\right)^2} \times \sum_i \left[f(c_{ij}(x_{ij})) \frac{\partial}{\partial x_{kl}} a_i(\mathbf{x}) + a_i(\mathbf{x}) \frac{\partial}{\partial x_{kl}} f(c_{ij}(x_{ij})) \right],$$

which can be simplified as

$$\frac{\partial}{\partial x_{kl}} a_i(\mathbf{x}) = -\frac{[a_i(\mathbf{x})]^2}{o_i} \sum_j \left[f(c_{ij}(x_{ij})) \frac{\partial}{\partial x_{kl}} b_j(\mathbf{x}) + b_j(\mathbf{x}) \frac{\partial}{\partial x_{kl}} f(c_{ij}(x_{ij})) \right],$$

$$\frac{\partial}{\partial x_{kl}} b_j(\mathbf{x}) = -\frac{[b_j(\mathbf{x})]^2}{d_j} \sum_i \left[f(c_{ij}(x_{ij})) \frac{\partial}{\partial x_{kl}} a_i(\mathbf{x}) + a_i(\mathbf{x}) \frac{\partial}{\partial x_{kl}} f(c_{ij}(x_{ij})) \right],$$

for $i, k = 1,2,...,I$, and $j,l = 1,2,...,J$.

There are $(I+J)\times I \times J$ equations which are linear with respect to the same number of unknowns, $\partial a_i(\mathbf{x})/\partial x_{kl}$ and $\partial b_j(\mathbf{x})/\partial x_{kl}$. Thus, the set of equations can be solved numerically. The partial derivatives can then be found by (6) to get the Jacobian matrix. The algorithm by Eckmann and Ruelle can now be used to calculate the Liapunov exponents for the doubly constrained gravity model. Liapunov exponents were calculated for the chaotic attractor shown in Fig. 5 and the result is $[0.1248\ -0.1449\ -0.3597\ -0.9477]$. The first one is positive, which confirms the attractor is chaotic.

B. Fractal dimensions

Fractal dimensions may be used to characterize the geometric feature of chaotic attractors. Several types of fractal dimension have been defined in the literature.[10] The main reason here for choosing one type of dimension over another is the ease and accuracy of its computation. The commonly used box-counting algorithm for calculating the fractal dimension is very inefficient.[10] The algorithm for computing the *correlation dimension* due to Grassberger and Procaccia[7] is more efficient and is therefore employed to estimate the correlation dimension for chaotic attractors in the gravity models.

The correlation dimension is defined based on the *correlation function* of an attractor. A correlation function is the average fraction of points within a certain radius ρ on the attractor. Let the sequence of N points $\{\mathbf{x}(1),\ldots,\mathbf{x}(n),\ldots,\mathbf{x}(N)\}$ be an orbit on an attractor in system (2). Then the correlation function $C(\rho)$ of the attractor is given by[10]

$$C(\rho) = \lim_{N\to\infty} \frac{1}{N^2} \{\text{The number of points } (\mathbf{x}(m),\mathbf{x}(n)) \text{ such that } |\mathbf{x}(m)-\mathbf{x}(n)| < \rho\}.$$

The correlation dimension D_C is defined as[10]

$$D_c = \lim_{\rho\to 0} \frac{\log\ C(\rho)}{\log\ \rho}.$$

In other words, it is the slope of the plot of $\log(C(\rho))$ versus $\log(\rho)$.

Using the above algorithm, the dimension for the chaotic attractor in Fig. 1 found in the unconstrained or singly constrained gravity model is calculated. The dimension estimated from the log–log plot of the correlation function is 1.8251, though the attractor lies in a three-dimensional state space. Also calculated is the correlation dimension for the chaotic attractor shown in Fig. 5 in the doubly constrained gravity model. The state space of this model is four dimensional. The slope of the log–log plot of the correlation function, or the correlation dimension, is found to be 1.653. These results mean that the dynamic gravity model is a *dissipative system*: the phase volume shrinks with time. The state space of the models considered above is three or four dimensional, but the evolution of the system is such that the final variations of O–D flows settle down in the state space to a region of dimension 1.7 or 1.8.

V. CONCLUSIONS

The dynamic gravity model has been investigated numerically in an attempt to identify different types of dynamic behavior in the model. Point attractors and period-2 attractors have been found to be the main feature in the models of lower dimensions. When the dimension is higher (3 or more for unconstrained or singly constrained model, and 4 or more for the doubly constrained model), period doubling, chaos, and other complicated bifurcations were found. The presence of chaos was confirmed by positive Liapunov exponents and fractal dimension. What behavior the system would exhibit in practice will depend on the values that the parameters can take. These parameter values are normally different for different geographical areas. For a particular area, empirical studies are needed to determine the type of model and the values of parameters in the model. Then we are able to find out if the system would stick to a stable equilibrium or if the behavior would be chaotic.

The significance of the results of the paper may be of twofold. First, it is important for transport planners and en-

gineers to be aware of the potential of irregular or chaotic behavior in the gravity model. It is also important to be aware that an equilibrium in the gravity model may not be unique and stable. Even though the unstable or chaotic behavior is not dominant in the system, it may occur temporarily as a result of disturbances caused by traffic incidence or accidents. It would be misleading to predict an O–D flow pattern (at a presumed equilibrium) from a static model when an underlying system is not at an equilibrium steady state. Secondly, when the system is in a chaotic regime, we cannot use the model to predict the future variations of the system as we normally do with a deterministic model. However, the variations will be confined in the region of the chaotic attractor, whose shape, position, and so on can be examined to get some idea on the variations and distributions of O–D flows in the state space. For example, here, the final variations of O–D flows in three- or four-dimensional systems were found to settle down in the state space to a region of dimension between 1 and 2. Further research should put more emphasis on the validation and calibration of the gravity model, and on finding out to what extent the form of deterrence functions and parameters values may be ''borrowed'' or transferred from one area to another. It would also be of interest to carry out theoretical analysis on the typical bifurcation sequence found in the unconstrained or singly constrained gravity model.

ACKNOWLEDGMENTS

The authors would like to thank Chris Wright, Mike Maher, and two anonymous referees for their constructive comments and suggestions on an earlier draft of this paper. The first author is grateful to Middlesex University for providing a studentship which supported the major part of the research described in this paper.

[1] J. de D. Ortuzar and L. G. Willumsen, *Modelling Transport* (Wiley, New York, 1990).
[2] D. S. Dendrinos and M. Sonis, *Chaos and Social-Spatial Dynamics* (Springer-Verlag, Berlin, 1990).
[3] D. F. Jarrett and X. Zhang, ''The dynamic behavior of road traffic flow: stability or chaos?'' *BCS Displays Group: Application of Fractals and Chaos*, edited by A. J. Crilly, R. A. Earnshaw, and H. Jones (Springer-Verlag, Berlin, 1993).
[4] X. Zhang and D. F. Jarrett, ''Traffic equilibrium in a dynamic trip assignment model and a dynamic gravity model,'' *Transportation Networks: Recent Methodological Advances*, edited by M. G. H. Bell (Elsevier, Oxford, 1998).
[5] J. M. T. Thompson and H. B. Stewart, *Nonlinear Dynamics and Chaos: Geometrical Methods for Engineers and Scientists* (Wiley, New York, 1988).
[6] R. Conte and M. Dubois, ''Liapunov exponents of experimental systems,'' *Nonlinear Evolutions*, edited by J. J. P. Leon (World Scientific, Singapore, 1988).
[7] P. Grassberger and I. Procaccia, ''Measuring the strangeness of strange attractors,'' Physica D **9**, 189 (1983).
[8] J.-P. Eckmann and D. Ruelle, ''Ergodic theory of chaos and strange attractors,'' Rev. Mod. Phys. **57**, 617 (1985).
[9] A. Wolf, J. B. Swift, H. L. Swinney, and J. A. Vastano, ''Determining Liapunov exponents from a time series,'' Physica D **16**, 285 (1985).
[10] T. S. Parker and L. O. Chua, *Practical Numerical Algorithms for Chaotic Systems* (Springer-Verlag, Berlin, 1989).